

Characterization of CO₃Ap-collagen Sponges Using X-ray High-resolution Microtomography

Departments of ¹Preventive Dentistry and ²Biomaterials Science, Hiroshima University School of Dentistry, 1-2-3 Kasumi, Minamiku, Hiroshima 734-8553, Japan

M. Itoh², A. Shimazu¹, I. Hirata², Y. Yoshida², H. Shintani², M. Okazaki²

For reconstruction and regeneration of hard tissues, scaffold biomaterials with large size pores and high porosity are important, in addition to their roles as supporting frames. To develop a new biodegradable scaffold biomaterial, CO₃Ap, which has crystallinity and a chemical composition similar to bone, was synthesized at pH 7.4 and 60 C. Then, the CO₃Ap was mixed with a neutralized collagen gel and the CO₃Ap-collagen mixtures with different kinds of CO₃Ap contents and porosity were lyophilized into sponges. Scanning electron micrography (SEM) observation of CO₃Ap-collagen sponges showed favorable pores for cell invasion. Approximately 50–300 μm size pores appeared to continue through the bulk. Higher magnification of the sponge showed a better adhesion between CO₃Ap crystals and collagen. X-ray high-resolution microtomography revealed a clear image of the 3D structure of the sponges. The porosity of 0, 70 and 90% (w/w) CO₃Ap-collagen sponges was 79.272.8%, 72.672.4% and 48.976.1%, respectively. The 70% (w/w) CO₃Ap-collagen sponge appeared to be the most favorable biomaterial from the viewpoint of natural bone properties. Mouse osteoblast MC3T3-E1 cells were cultured in aMEM with 10% FCS for 2 weeks. Hematoxylin–eosin staining confirmed osteoblast cells invaded well into the CO₃Ap-collagen sponge. These sponges are expected to be used as hard tissue scaffold biomaterials for therapeutic uses.

Keywords; bone repair, collagen, hydroxyapatite composite, scaffold.

Introduction

Various kinds of materials: ceramics, metals, polymers and their composites were considered as bone substituting materials [1–4]. In particular, many different kinds of hydroxyapatites (HAp) and other calcium phosphates such as tricalcium phosphate (TCP) [5], dicalcium phosphate dihydrate (DCPD) [6], octacalcium phosphate (OCP) [7], tetracalcium phosphate (4CP) [8] have been studied because they are composed mainly of calcium and phosphate, as are bone and teeth. Synthetic HAp have been eagerly investigated and applied as hard tissue biomaterials for many years, because of their good biocompatibility [9,10]. Mostly, sintered Haps were developed as representatives of bone and tooth roots. Conventional block-type HAp, however, is difficult to process into complex forms, and granular-type HAp, which is injected into the resorbed place with NaCl solution, does not readily retain the required form. Porous calcium phosphates were developed from the viewpoint of cells penetrating into the materials. They showed a relatively good bonding to natural bone [11]. Unfortunately, however, these HAp were permanent non-metabolized materials, and those porous and non-porous block-type hard materials had a brittle nature, even if laminated by metals [12,13], and they had the possibility of cracking or exerting a long-term influence on the surrounding tissues since they remained in the body without metabolizing. Therefore, the recent focus has been on biodegradable materials [14–19].

To obtain better handling properties, apatite-collagen/gelatin composites have been developed [14–16,19]. We have synthesized CO3Ap, which has a similar crystallinity to that of bone and succeeded in making CO3Ap-collagen composite with a collagen whose antigenicity had been removed by enzymatic treatment [14,15]. These CO3Ap-collagen composites showed good biocompatibility when implanted into the abdomen and beneath the periosteum cranii of rats. However, these composites had no space in the inner bulk for the cell to invade. Recently, tissue engineering has been developed and porous hard tissue biomaterials are expected [20]. To invade into the inner core of the materials, these materials need a much larger pore size than that of osteoblasts with approximately 10- μ m diameters of average size without consideration of the deformation and projection length, since osteoblasts sometimes deform with their expanded projections and become less likely to invade into the deeper core by adhering to the walls of pores. Thus, in this study we investigated CO3Ap-collagen sponges with larger pores, in which osteoblasts can both easily invade and remain.

On the other hand, the use of X-ray as a nondestructive tool for investigating the internal structure of materials at the micron scale has grown rapidly over the past decade as a result of the advent of synchrotron radiation sources [21–25]. In a typical computed microtomography (CMT) experiment, a sample is illuminated by a collimated beam of X-rays, and data is collected for multiple sample orientations using a charge-coupled device. A time-consuming

reconstruction process is used to obtain three-dimensional (3D) raw data with a spatial resolution of as little as 1 mm. The 3D image contains quantitative information on the X-ray attenuation coefficient at particular X-ray energy levels. In this study, to clarify the 3D image of CO3Apcollagen sponge samples, the material characteristics were examined by microtomography with soft X-rays.

Materials and methods

Synthesis of CO₃apatite

Carbonate apatite (CO₃Ap) was synthesized at 6071 C and pH 7.470.2. A 0.5 l solution of 100 mmol/l Ca(CH₃COO)₂ · H₂O and a 0.5 l solution of 60 mmol/l NH₄H₂PO₄ containing 60 mmol/l (NH₄)₂CO₃, were fed into a mechanically stirred solution of 1.3 mol/l acetate buffer. The suspension was stirred for 3 h, then kept at 25 C for 24 h. The CO₃Ap was separated by filtration, washed with distilled water, and dried at 60 C. Well-crystallized HAp was also synthesized at 6071 C in the same manner without carbonate.

Identification and chemical analysis

X-ray diffraction was employed to identify precipitates and estimate the degree of crystallinity. Measurements were made on an Ultima+ model RigakuDenki X-ray diffractometer with graphite-monochromatized CuK α radiation at 40 kV, 30 mA. Scanning electron micrography (SEM) of crystals were obtained using a HITACHI S-4100 apparatus. Calcium concentrations were determined using an atomic absorption spectrophotometer (ShimadzuAA-6400). Each 50 mg of CO₃Ap and HAp (n 1/4 5) was dissolved perfectly in 0.1 n HCl solution and total phosphate concentrations were determined by UV spectrophotometry [26]. Each 10 mg of CO₃Ap sample (n 1/4 5) was taken into the Conway dish and carbonate concentrations were determined by the titration method of Conway [27].

Preparation of CO₃Ap-collagen sponges

First, 0.5 wt% of calf skin collagen solution (Cellgen; Koken Co. Ltd., Japan), which had been treated by application of enzymes to minimize antigenicity, was neutralized with 0.05 n NaOH, then mixed immediately with 0–90%(w/w) CO₃apatite by dry weight. The mixture gels were put into 96-well culture plates. Then, the plates were frozen at -80 C for 2 h and dried in a freeze dry machine (EYELA Co. Ltd., Japan) for 24 h. The sponges were subjected to UV radiation for 4 h, placed 10 cm from the UV lamp (10 W, 253.7 nm), to become insoluble. 2.4. mCT observation Each 6mmf 10mm cylindrical sample of the CO₃Ap-collagen sponges (Fig. 1) was set on the sample holder with adhesive tape and measured with an X-ray high-resolution microtomograph, mCT SKYSCAN 1072 (SkyScan Co. Ltd., Belgium) with detection ability of 2 mm at 80 kV and 100 mA. The microtomograph was reconstructed to a 3D image. The porosity of the composites was calculated from the 3D data.

Culture of osteoblasts

Mouse osteoblast MC3T3-E1 cells derived from untransformed mouse bone marrow were obtained from RIKEN Cell Bank (Tsukuba, Japan) and were maintained in a continuous culture at 37 C in a 5% CO₂ humidified atmosphere. Cells were grown in Dulbecco's Modified Eagle Medium (DMEM) solution

supplemented with 10% heat-inactivated FBS. Penicillin (100 U/ml) and streptomycin (100 mg/ml) were added to the media. To examine the degree of cell invasion, mouse MC3T3-E1 cells were grown for 2 weeks in minimum essential medium alpha modification (αMEM) with 10% heat-inactivated FBS in 96-well plates containing the CO3Ap-collagen sponges and (5×10^4 cells/well; n 1/4 5) at 37 C in a 5% humidified atmosphere. Finally, the sponges with cells were embedded in paraffin, crosssectioned, and stained with hematoxylin–eosin for histological examination under a light microscope.

Results

Synthetic CO3Ap had a poorly crystallized apatitic pattern similar to that of human bone (Fig. 2) with the composition of Ca=8.9470.04 mmol/g, total P=5.1370.10 mmol/g and CO3=0.6970.05 mmol/g, compared with that of well-crystallized HAp, which was synthesized at 60 C.

The pore size of 100%(w/w) collagen without CO3Ap increased with the increase of water content in the preparation gels, i.e., with the concentration of collagen. Fig. 3 shows the SEM of the typical 0, 70 and 90%(w/w) CO3Ap-collagen sponges prepared by lyophilizing, compared with the dense 0, 70 and 90%(w/w) CO3Ap-collagen composite made by the same method of previous preparations [14,15]. Collagen film (Fig. 3A) showed a smooth surface compared with 70%(w/w) (Fig. 3B) and 90%(w/w) (Fig. 3C) CO3Ap-collagen composites, which showed compacted apatite crystals. On the other hand, the pure collagen sponge (Fig. 3D) showed a highly porous structure. Approximately 50–300 μ m size pores appeared to continue deep into the sponge. The coagulated CO3Ap crystals were observed with the fibrous ribbons of collagen for CO3Ap-collagen sponge. The 70%(w/w) CO3Ap-collagen sponge (Fig. 3E) showed favorable pore sizes, in which the cells could invade easily. In general, large pores such as several hundreds μ m are required to the invasion of the cells [28]. The pore size of the 90%(w/w) CO3Ap-collagen sponge (Fig. 3F) appeared to be smaller than those of the 70%(w/w) CO3Ap-collagen sponge. Higher magnification of the sponge suggested a better familiarity between CO3Ap crystals and collagen (Fig. 4).

Fig. 5 shows 2D images of the composite sponges observed by X-ray high-resolution microtomography. The center of the wave patterns indicates the X-ray absorption. Since pure collagen (0%(w/w) CO3Ap-collagen) sponge was X-ray translucent, a clear image could not be observed. The 90%(w/w) CO3Ap-collagen sponge showed a deep non-translucent image, which suggested the existence of many X-ray impenetrable CO3Ap crystals.

Fig. 6 shows the 2D cross-sectional images of the CO3Ap-collagen sponges. Since pure collagen was translucent, sensitivity was increased (Fig. 6A). When these 2D cross-sectional images were reconstructed, 3D images of the sponges could be displayed (Fig. 7). The 3D pore image of each sponge was clearly observed. The computer software was able to calculate the porosity of the composite sponges. The porosity of 0, 70, 90%(w/w) CO3Ap-collagen sponges was 79.272.8%, 72.672.4% and 48.976.1% (n 1/4 5), respectively.

When osteoblast MC3T3-E1 cells were cultured in the culture well with the sponges after 2-weeks, the histological stain with hematoxylin–eosin showed many osteoblasts had penetrated into the inner part of the sponge (Fig. 8). There was no significant difference in the invading osteoblast quantity between the 5 samples examined.

Discussion

Until now, a number of HAPs have been used as bone substituting materials. However, most of them were permanent and remained in the body. Recently, use of CO₃Ap has focused on their biodegradability. The present CO₃Ap-collagen sponge and the previous composite [14,15] were similar to bone and biodegradable. FGMgCO₃Ap-collagen composite [29] showed relatively faster metabolization than CO₃Ap-collagen composite beneath the periosteum cranii of rats. Crystallinity and CO₃ content are important for biodegradability. The crystallinity of bone apatites is poor and soluble, and easy to metabolize. Furthermore, CO₃ content of bone apatite is 4–6%(w/w) [30]. Many different kinds of calcium phosphates, in addition to carbonate apatites, have been investigated. If the Ca/P ratio and/or chemical composition of implanted materials such as other calcium phosphates: TCP, OCP or 4CP are significantly different from those of bone, other components, which must be digested in the human body, will remain and excess phosphate of TCP compared with CO₃Ap sometimes appeared to affect the tissues around the implanted materials. Therefore, it is suggested that CO₃Ap with a chemical composition similar to bone is desirable.

Furthermore, human hard tissues are composed of CO₃Ap and collagen, which contribute to bind apatite crystals. In general, osteoclasts and osteoblasts invade the bone matrix in association with blood vessels.

Osteoclasts erode bone matrix, while osteoblasts secrete bone matrix [31,32]. Freshly formed material consisting chiefly of type I collagen, the so-called osteoid, is rapidly converted into hard bone matrix by the deposition of calcium phosphate crystals within it [32]. Therefore, from the viewpoint of bone mineralization in vivo, prior preparation of collagen matrix is very useful for mineralization. However, the mechanisms controlling the initiation of mineralization of bone matrix are still not clear. The extracellular matrix such as collagen may contribute to form the morphology of bone together with apatite crystals. In the present case, the space in which the extracellular matrix forms, and also the porosity or pore size are important because the osteoblast cells sometimes expand projections and change the features. Then, the cells expand to several times their original size. The projection attaches to the surrounding collagen fibers and the cells accumulate mineral components such as calcium and phosphates and form HAP crystals as a matrix vesicle (MV). In this process, the existence of collagen is important which is why in this study the collagen sponge was adopted as a bone matrix. In addition, the CO₃Ap-collagen sponges in this study were biodegradable similar to the CO₃Ap-collagen composites reported previously [14,15], although the rate of biodegradability was different for each in relation to the porosity.

SEM showed approximately 50–300 μm pores, which appeared to be favorable for cell penetration. The pore size and distribution of the 70%(w/w) CO₃Ap-collagen sponge was similar to that of pure collagen. The difference of

mCT estimated porosity between pure collagen (79.272.8%) and CO3Ap-collagen sponge (72.672.4%) was not significantly different, although the porosity of the 90%(w/w) CO3Ap-collagen sponge (48.976.1%) decreased. When considering that natural bone contains approximately 60–70%(w/w) of CO3apatite, and similar 60–70%(w/w) CO3Ap-collagen sponges are acceptable for therapeutic use.

There is a long history of imaging with X-rays. 3D Xray imaging was developed in the 1960s and 1970s [22]. Recently, mCT tomography was often used in the medical and dental fields. With the introduction of synchrotron X-ray sources, hard X-rays are available at a few micron resolutions, while nanotomography was developed with soft X-rays for imaging biological and microfabricated objects at 10–100nm resolutions and currently is routinely used in microtomography [23–25]. mCT is different from the conventional CT scanner typically used in the industry, which has a very strong transmission ability. Therefore, conventional hard CT can hardly detect the organic materials and porous materials such as CO3Ap-collagen sponges used in the present study. However, we could successfully construct the 3D image of CO3Ap-collagen sponges using soft Xray high-resolution microtomography. Hematoxylin–eosin staining for the cell assay was able to confirm the penetration of the cells into the sponge and the effectiveness of the porosity. In conclusion, it is suggested that the CO3Ap-collagen sponge developed in the present study could possibly be used for therapeutic purposes. Further cell culture and animal experiments are currently in progress.

References

- [1] Hench LL, Splinter RJ, Allen WC, Greelee TK. Bonding mechanisms at the interface of ceramic prosthetic materials. *J Biomed Mater Res Symp* 1971;2:117–41.
- [2] Linkow LI, Chercheve P. Theories and techniques of oral implantology. Saint Louis: CV Mosby; 1970.
- [3] Oka M, Ushio K, Kumar P, Ikeuchi K, Hyon SH, Nakamura T, Fujita H. Development of artificial cartilage. *Eng Med* 2000;214H:59–68.
- [4] Heikkila JT, Aho AJ, Kangasniemi I, Yli-Urpo A. Polymethylmethacrylate composites: disturbed bone formation at the surface of bioactive glass and hydroxyapatite. *Biomaterials* 1996;17: 1755–60.
- [5] Gregory TM, Moreno EC, Patel JM, Brown WE. Solubility of β - $\text{Ca}_3(\text{PO}_4)_2$ in the system $\text{Ca}(\text{OH})_2$ – H_3PO_4 – H_2O at 5, 15, 25 and 37.5 C. *J Res Natl Bur Stand* 1974;78A:667–74.
- [6] Tung MS, Chow LC, Brown WE. Hydrolysis of dicalcium phosphate dihydrate in the presence or absence of calcium fluoride. *J Dent Res* 1985;64:2–5.
- [7] Brown WE, Eidelman N, Tomazic B. Octacalcium phosphate as a precursor in biomineral formation. *Adv Dent Res* 1987;1: 306–13.
- [8] Brown WE, Epstein EF. Crystallography of tetracalcium phosphate. *J Res Natl Bur Stand (US)* 1965;69A:547–51.
- [9] Nery EB, Lynch KL, Hirthe WM, Mueller KH. Bioceramic implant in surgically produced infrabony defects. *J Periodontol* 1975;46:328–47.
- [10] Rothstein SS, Paris DA, Zacek MP. Use of hydroxyapatite for the augmentation of deficient alveolar ridges. *J Oral Maxillofac Sug* 1984;42:224–30.
- [11] Kenny EB, Lekovic V, Sa Ferreira JC, Han T, Dimitrijevic B, Carranza Jr. FA. Bone formation within porous hydroxyapatite implants in human periodontal defects. *J Periodontol* 1986;57: 76–83.
- [12] Keller L, Dollase WA. X-ray determination of crystalline hydroxyapatite to amorphous calcium-phosphate ratio in plasma sprayed coatings. *J Biomed Mater Res* 2000;49:244–9.
- [13] Zeng H, Lacefield WR. The study of surface transformation of pulsed laser deposited hydroxyapatite coatings. *J Biomed Mater Res* 2000;50:239–47.
- [14] Okazaki M, Ohmae H, Hino T. Insolubilization of apatite/collagen composites by UV irradiation. *Biomaterials* 1989;10: 564–8.
- [15] Okazaki M, Ohmae H, Takahashi J, Kimura H, Sakuda M. Insolubilized properties of UV-irradiated CO_3 apatite-collagen composites. *Biomaterials* 1990;11:568–72.
- [16] Ten Huisen KS, Brown PW. The formation of hydroxyapatite/gelatin composites at 38 C. *J Biomed Mater Res* 1994; 28:27–33.

- [17] Constantz BR, Ison IC, Fulmer MT, Poser RD, Smith ST, VanWagoner M, Ross J, Goldstein SA, Jupiter JB, Rosenthal DI. Skeletal repair by in situ formation of the mineral phase of bone. *Science* 1995;267:1796–9.
- [18] Tanahashi M, Kokubo T, Nakamura T, Katsura Y, Nagano M. Ultrastructural study of an apatite layer formed by a biomimetic process and its bonding to bone. *Biomaterials* 1996;17:47–51.
- [19] DuC, Cui FZ, Zhang W, Feng QL, ZhuXD, de Groot K. Formation of calcium phosphate/collagen composites through mineralization of collagen matrix. *J Biomed Mater Res* 2000;50:518–27
- [20] Ohgushi H, Goldberg VM, Caplan AI. Heterotopic osteogenesis in porous ceramics induced by marrow cells. *J orthop Res* 1989;7:568–78.
- [21] National center for microscopy and imaging research. <http://www-ncmir.ucsd.edu/CMDA/>.
- [22] von Laszewski G, Insley JA, Foster I, Bresnahan J, Kesselman C, Su M, Thiebaut, Rivers ML, Wang S, Tieman B, McNulty I. Real-time analysis, visualization, and steering of microtomography experiments at photon sources. <http://www.mcs.anl.gov/Xray>.
- [23] Lehr J. 3D X-ray microscopy: tomographic imaging of mineral sheaths of bacteria *Leptothrix ochracea* with the Göttingen X-ray microscope at BESSY. *Optik* 1997;104:166–70.
- [24] Wang Y. Three-dimensional imaging in soft X-ray microscopy. Ph.D. thesis, Department of Physics & Astronomy, State University of New York at Stony Brook, 1998.
- [25] Haddad WS, McNulty I, Trebes JZ, Anderson EH, Levesque RA, Yang L. Ultra high resolution X-ray tomography. *Science* 1994;266:1213–5.
- [26] Eastoe JE. Method for the determination of phosphate calcium and protein in small portions of mineralized tissues. Liege: Universite de Liege; 1965.
- [27] Conway EJ. Microdiffusion analysis and volumetric error, 3rd ed. New York: Van Nostrand; 1950.
- [28] Ohgushi H, Caplan A. Stem cell technology and bioceramics: from cell to gene engineering. *J Biomed Mater Res (Appl Biomater)* 1999;48:913–27.
- [29] Yamasaki Y, Yoshida Y, Okazaki M, Shimazu A, Uchida T, Kubo T, Akagawa Y, Hamada Y, Takahashi J, Matsuura N. Synthesis of functionally graded MgCO₃apatite accelerating osteoblast adhesion. *J Biomed Mater Res* 2002;62:99–105.
- [30] Miles AEW In: . Structural and chemical organization of teeth, Vol. II. New York: Academic Press; 1967.
- [31] Noda M. Cellular and molecular biology of bone. San Diego: Academic Press; 1993.
- [32] Albert B, Bray D, Lewis J, Raff M, Roberts K, Watson JD. Molecular Biology of the Cell. 3rd ed. New York: Garland Publishing; 1994. p. 949–1010.

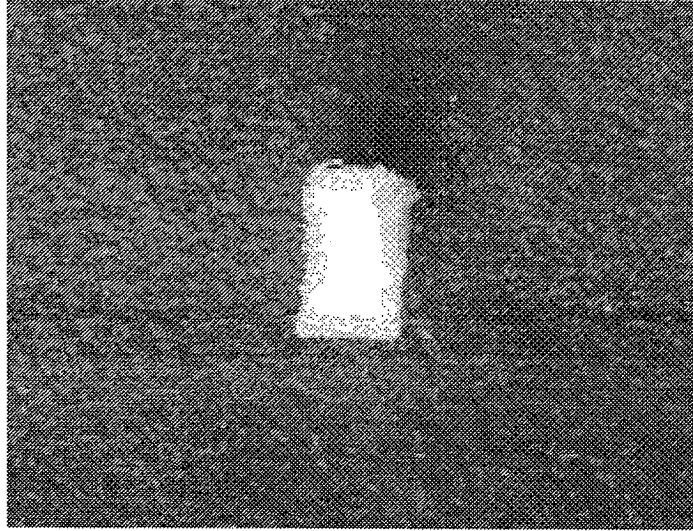
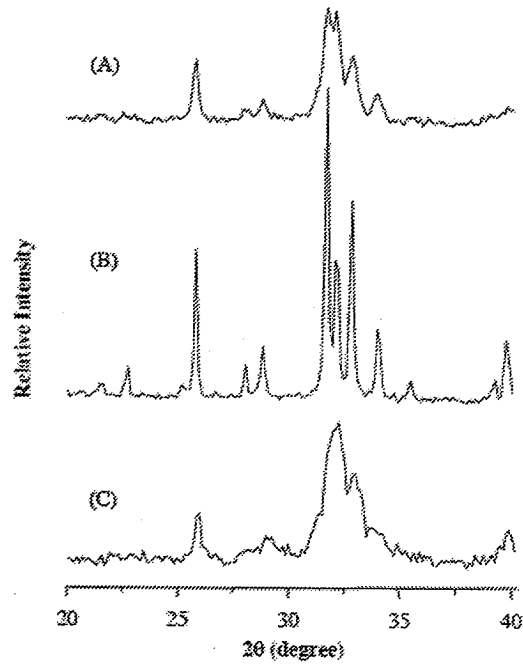


Fig. 1. CO₂Ap-collagen sponge sample with higher porosity with respect to the inversion of cells.



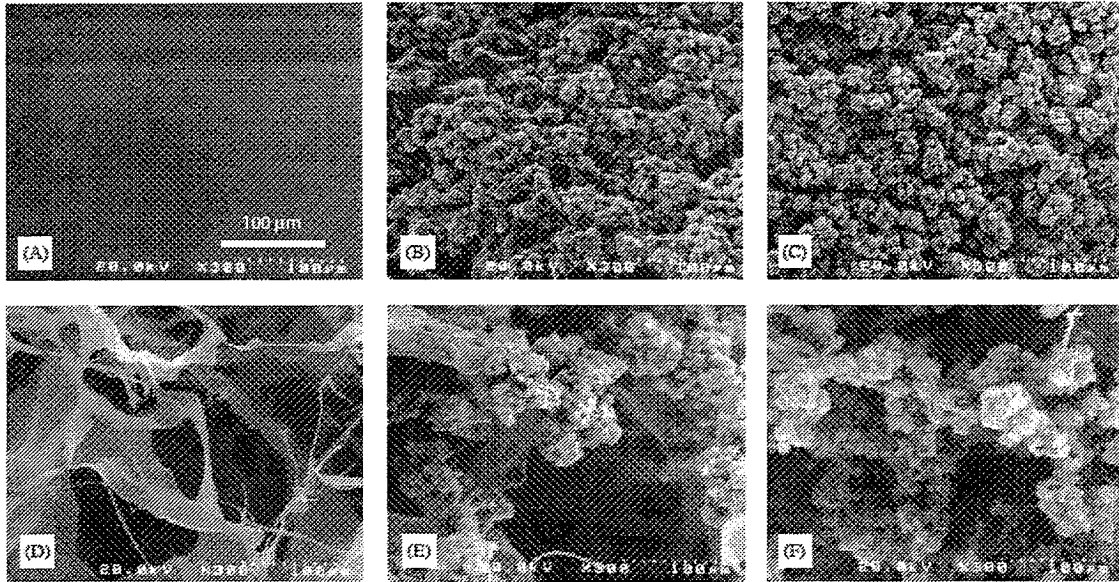


Fig. 3. Pure collagens (A, D), 70%(w/w) (B, E) and 90%(w/w) (C, F) CO_3Ap -collagen composites and sponges. The above film and composites were constructed with the conventional method of centrifugation without lyophilization. A: film; B, C: composites; D, E, F: sponges.

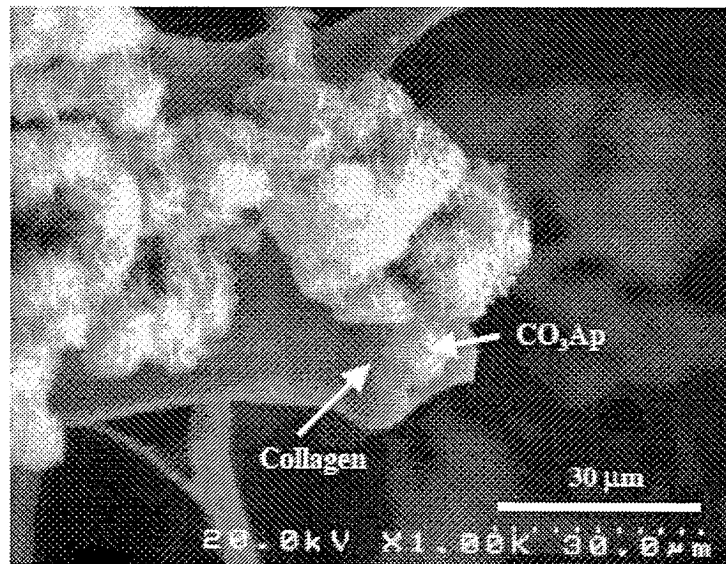


Fig. 4. SEM photo of 70%(w/w) CO_3Ap -collagen sponge with higher magnification. Photo shows the familiarity between CO_3Ap crystals (Ap) and collagen (Co).

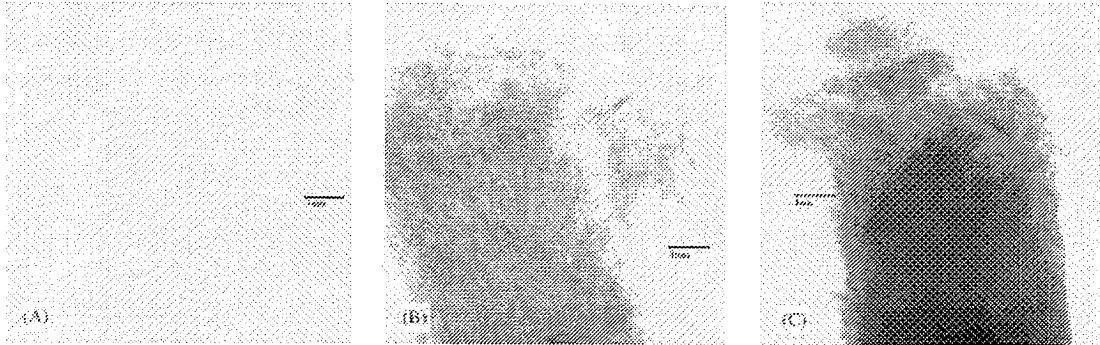


Fig. 5. Microtomographic images of pure collagen (A), 70%(w/w) (B) and 90%(w/w) (C) CO_3Ap -collagen sponges. Non-translucent images revealed clearly with the increase of CO_3Ap crystal content.

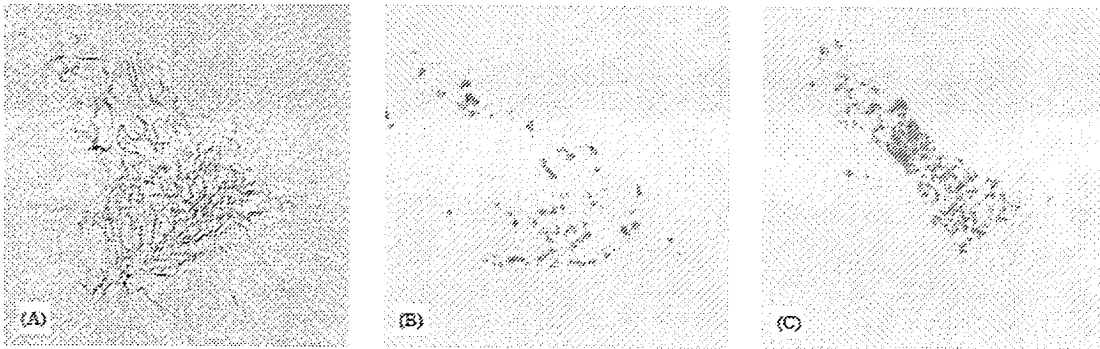


Fig. 6. 2D cross-sectional images of pure collagen (A), 70%(w/w) (B) and 90%(w/w) (C) CO_3Ap -collagen sponges.

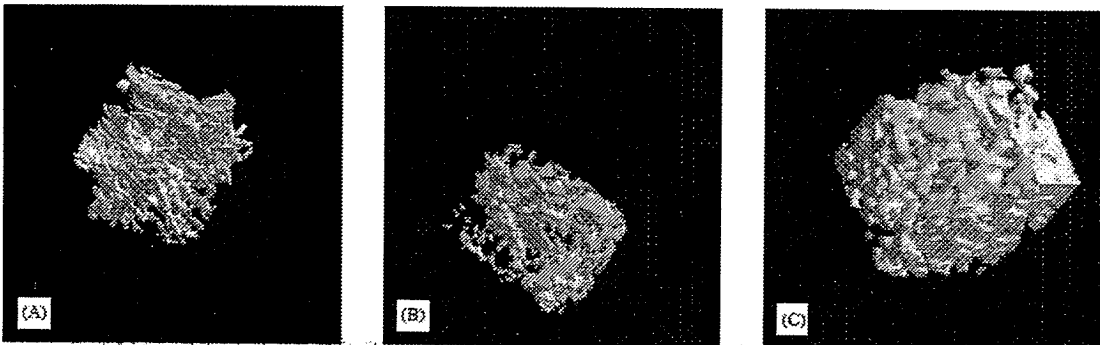


Fig. 7. 3D microtomographic images of pure collagen (A), 70%(w/w) (B) and 90%(w/w) (C) CO_3Ap -collagen sponges.

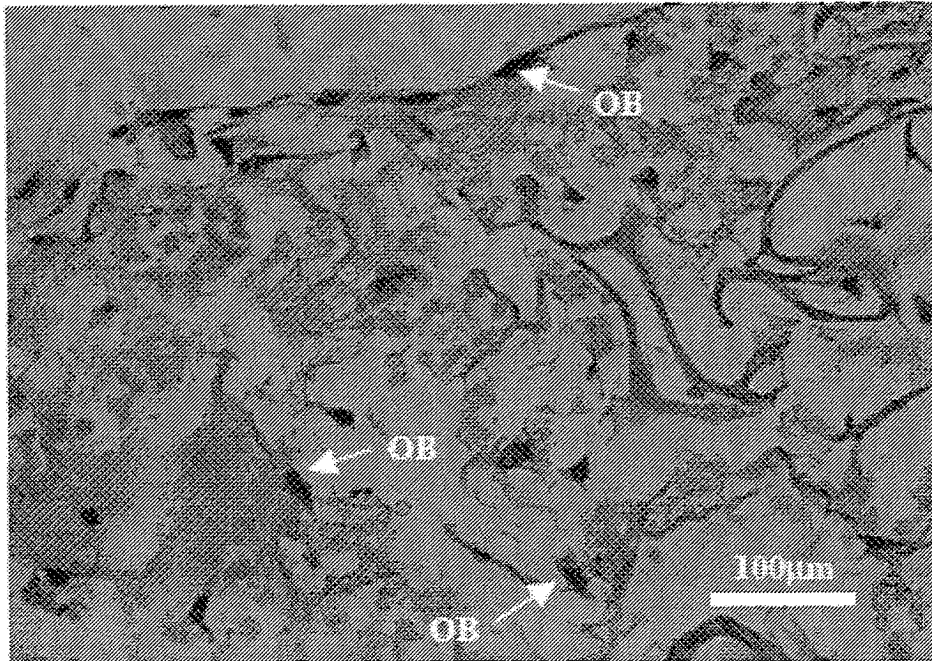


Fig. 8. Histological observation of osteoblasts in the 70%(w/w) CO₃Ap-collagen sponge cultured for 2 weeks with H-E staining.